The Abdus Salam International Centre for Theoretical Physics

United Nations Educational, Scientific and Cultural Organization

IAEA International Atomic Energy Agency

2051-1

Workshop on High Resolution Climate Modelling

10 - 14 August 2009

Projection of Changes in Weather Extremes Using MRI/JMA Super High-Resolution Atmospheric Models

KITOH Akio

Meteorological Research Institute
Climate Research Department 1-1 Nagamine,Tsukuba
Ibaraki 305-0052
JAPAN

Projection of Changes in Weather Extremes Using MRI/JMA Super High-Resolution Atmospheric Models

Akio KITOH

Meteorological Research Institute, Tsukuba, Japan

Needs for high resolution models for adaptation studies

• representation of topography depends on resolution (land-sea distribution, mountain height, snow-rain threshold, …)

• low resolution models often fail to reproduce precipitation systems such as tropical cyclones, stationary front systems and blocking

• high resolution models have better mean climate

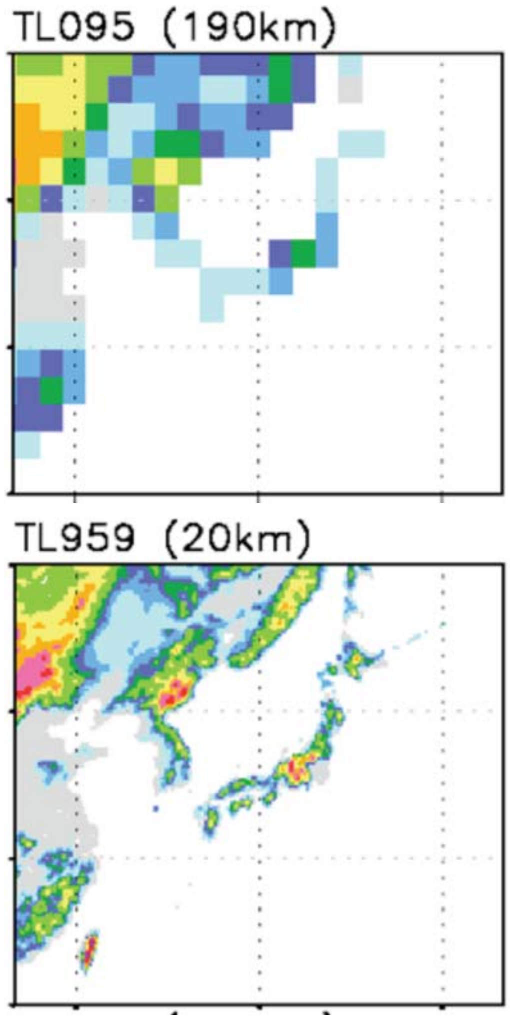

MRI/JMA Atmospheric GCM

- JMA : Operational global NWP model from Nov 2007
- MRI : Next generation climate model
- Based on operational JMA-GSM
- Resolution: TL959(20km) with 60 layers
- Time integration: Semi-Lagrangian Scheme (Yoshimura, 2004)
- Physics
  - SW radiation: Shibata & Uchiyama (1992)
  - LW radiation: Shibata & Aoki (1989)
  - Cumulus convection: Prognostic Arakawa-Schubert (Randall and Pan, 1993)
  - Land hydrology: MJ-SiB: SiB with 4 soil-layers and 3 snow-layers
  - Clouds: large-scale condensation, Cumulus, stratocumulus
  - PBL: Mellor & Yamada (1974,1982) level-2 closure model
  - Gravity wave drag: Iwasaki et al. (1989) + Rayleigh friction

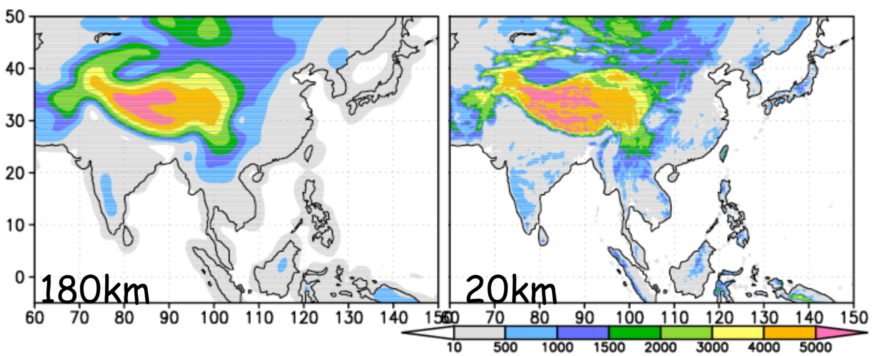

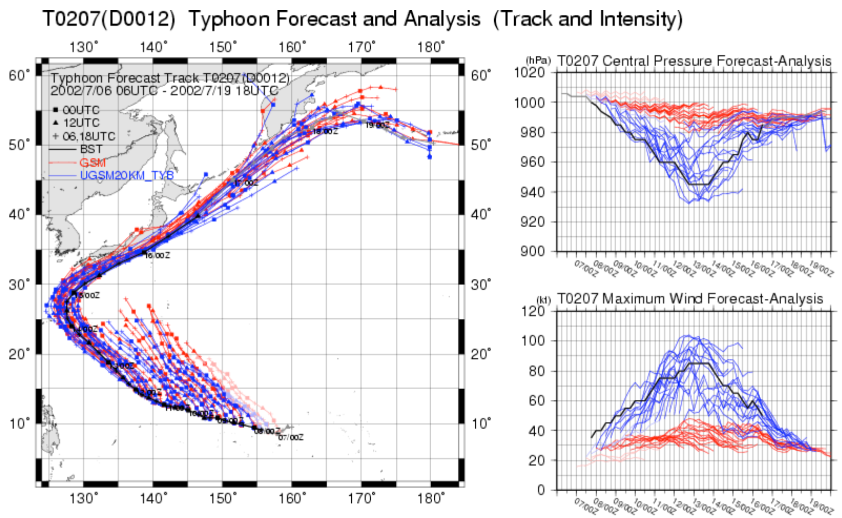

Kakushin Team-Extremes Time-Slice Experiments

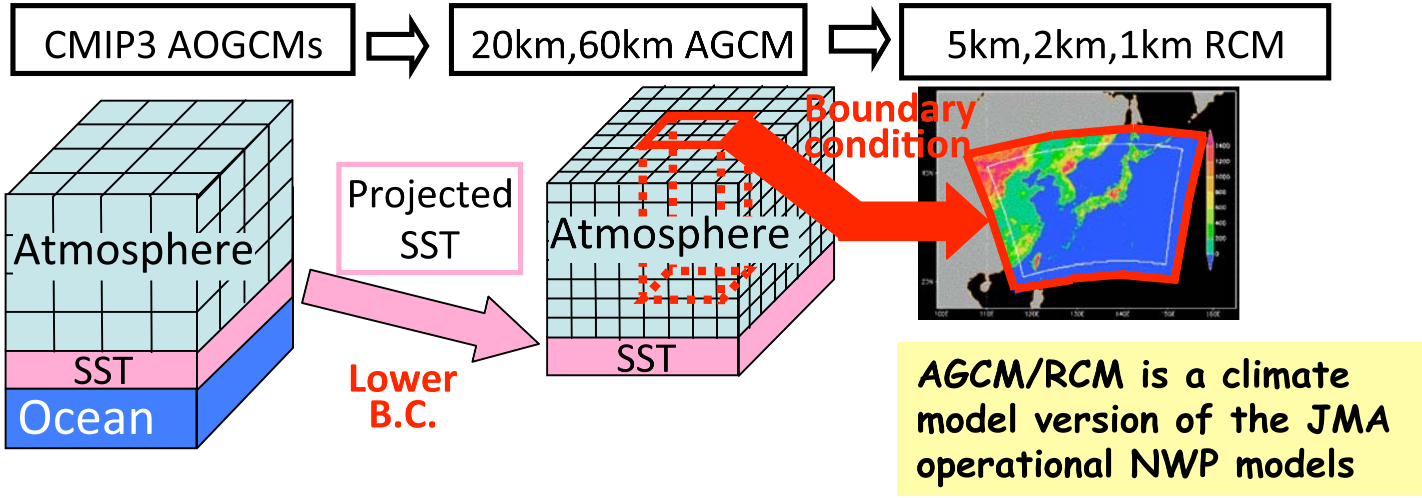

- Present-day (1979-2003)
  - the observed sea surface temperature (SST) and sea-ice concentration
- Near Future (2015-2039) and Future (2075-2099)
  - the SST and sea-ice anomalies of the CMIP3 multi-model ensemble mean are added to the observations, retaining the present interannual variability

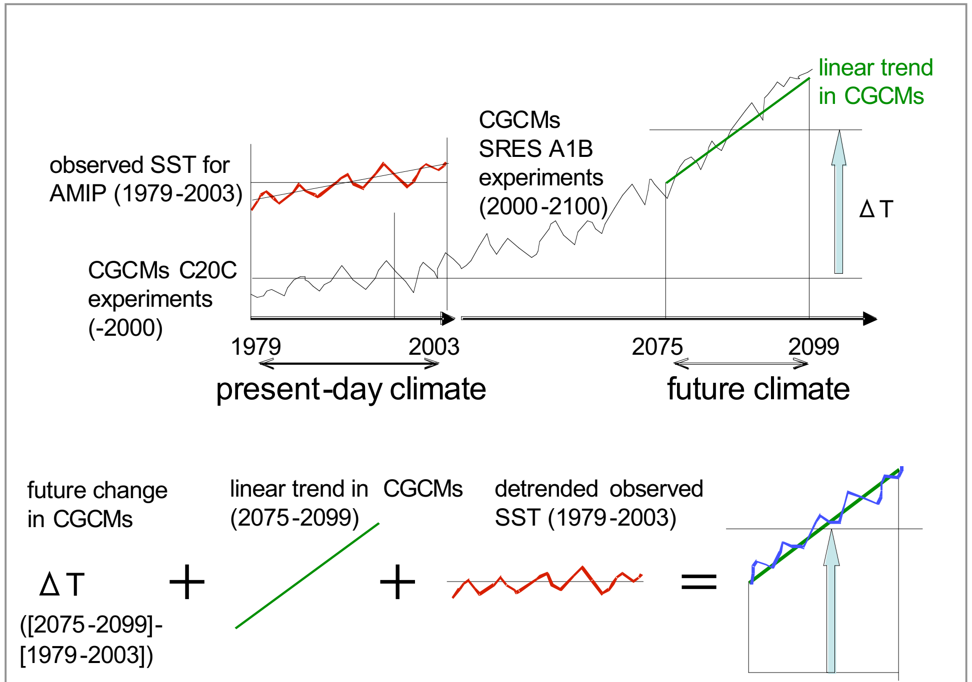

Mizuta et al. (2008)

Use of one-member 20-km AGCM run and ensemble runs with 60-km AGCM

period	SST	initial condition 0	initial condition 1	initial condition 2
Present: 1979-2003	observation	HP0A	HP0A_m01	HP0A_m02
Future: 2075-2099	CMIP3 average	HF0A	HF0A_m01	HF0A_m02
	MRI-CGCM2.3.2	HF0A_mri	HF0A_mri_m01	HF0A_mri_m02
	MIROC_hires	HF0A_miroch	HF0A_miroch_m01	HF0A_miroch_m02
	CSIRO	HF0A_csiro	HF0A_csiro_m01	HF0A_csiro_m02

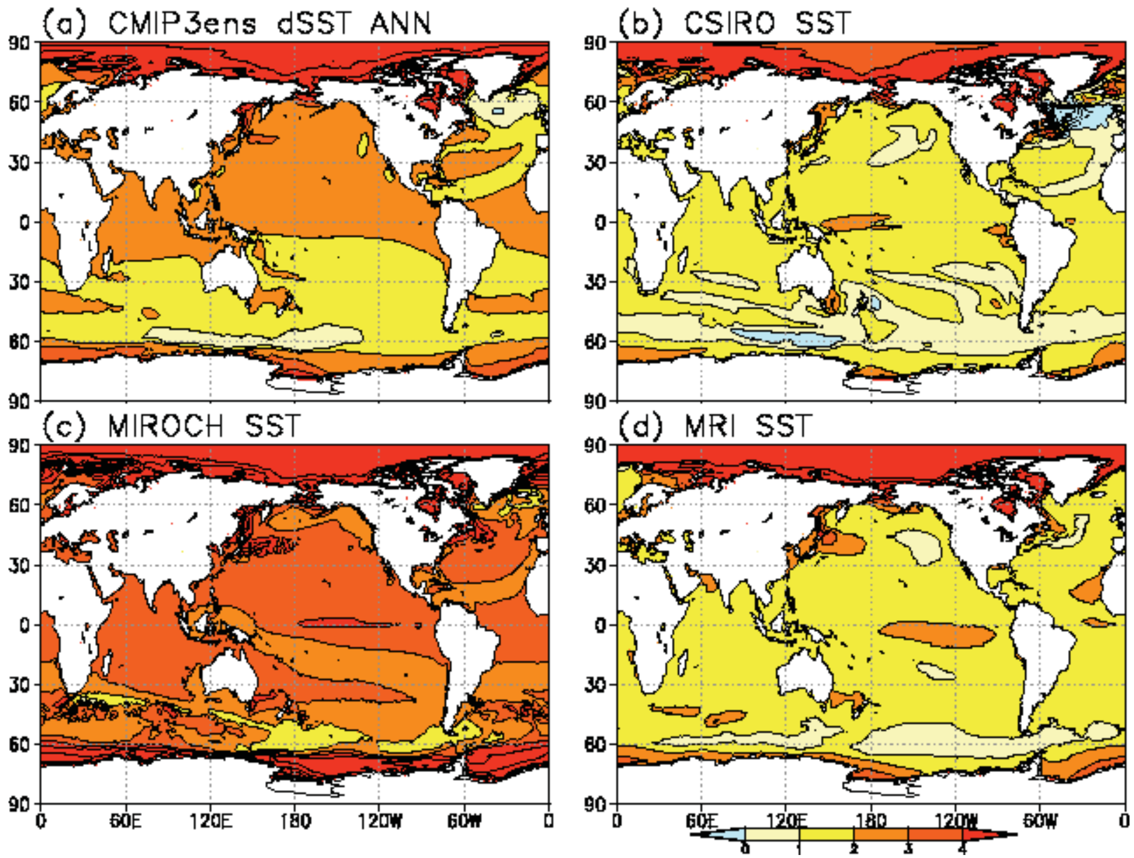

- 20-km mesh model is expensive, hard to run many cases, and thus hard to say about uncertainty of the results
- 60-km mesh model can be used to assess statistical significance of regional climate changes

Validation: Inter-annual variation of TC frequency

Observation

20-km AGCM (AMIP run 1979-2003)

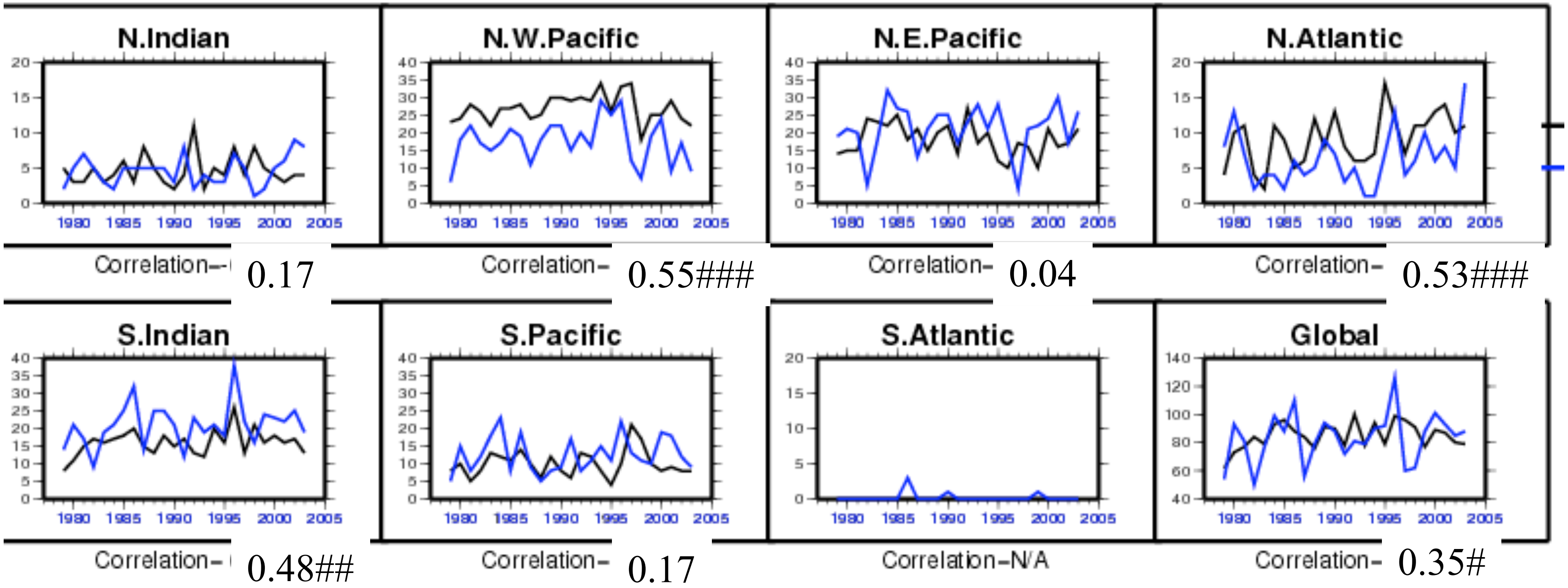

###:99% significance level
##:95% significance level
#:90% significance level

There is a skill for TC frequency interannual variation associated with ENSO

Number of TC Generated in Each Latitude

Annual global average
Present =82 (Observation:84)
Future =66 (20% decrease)

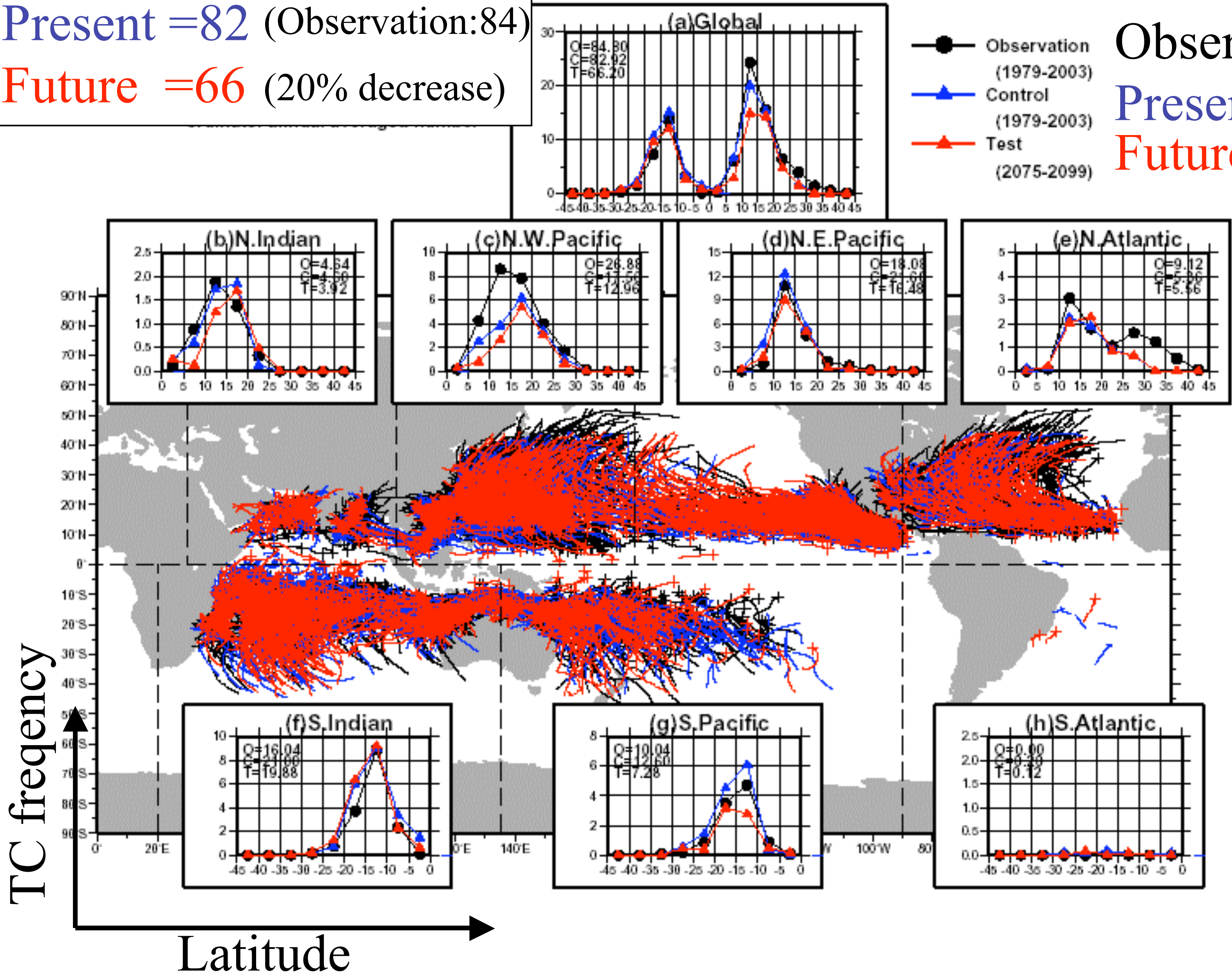

Observation
Present-day(25yr)
Future(25yr)

TC intensity

Change in TC intensity and duration

Intensity

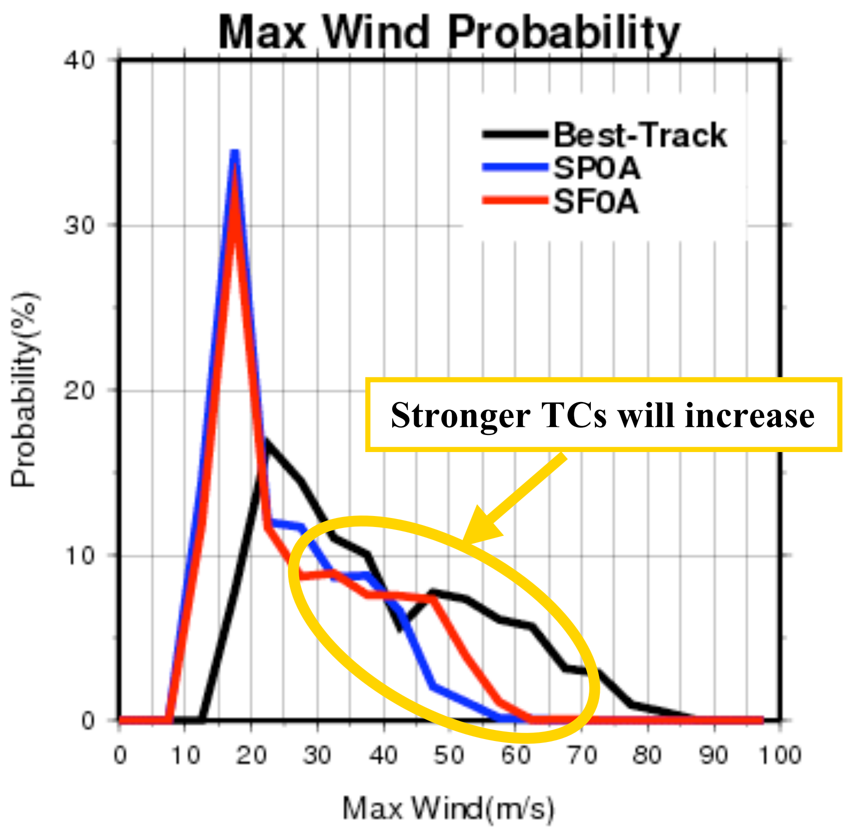

Duration when wind speed is over 17m/s

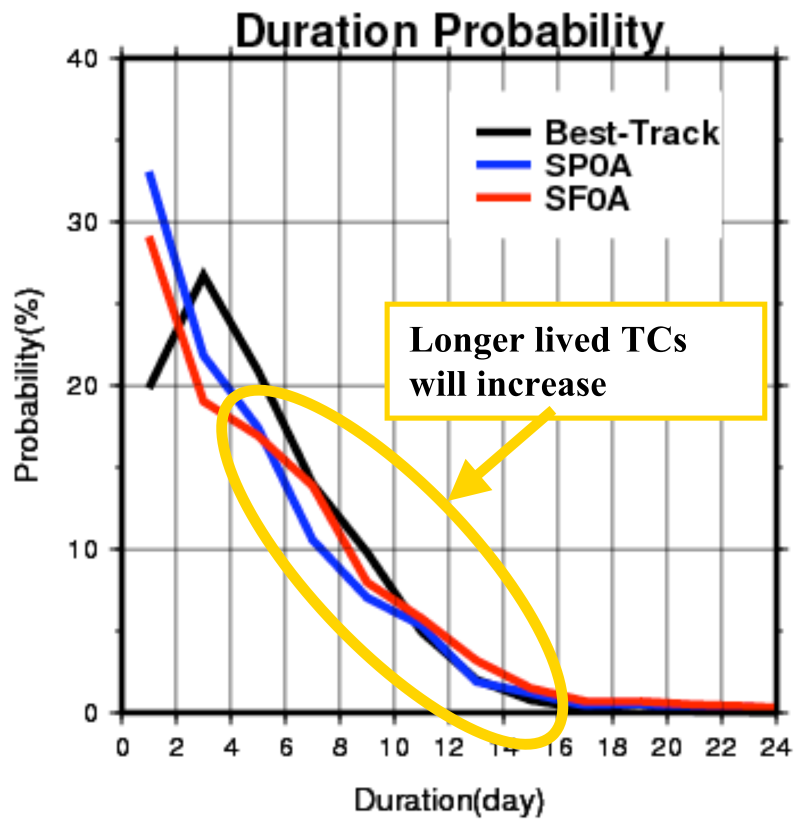

Observation

Present Experiment

Future Experiment

Radial Profile Change around TC

Precipitation | **Surface Wind**

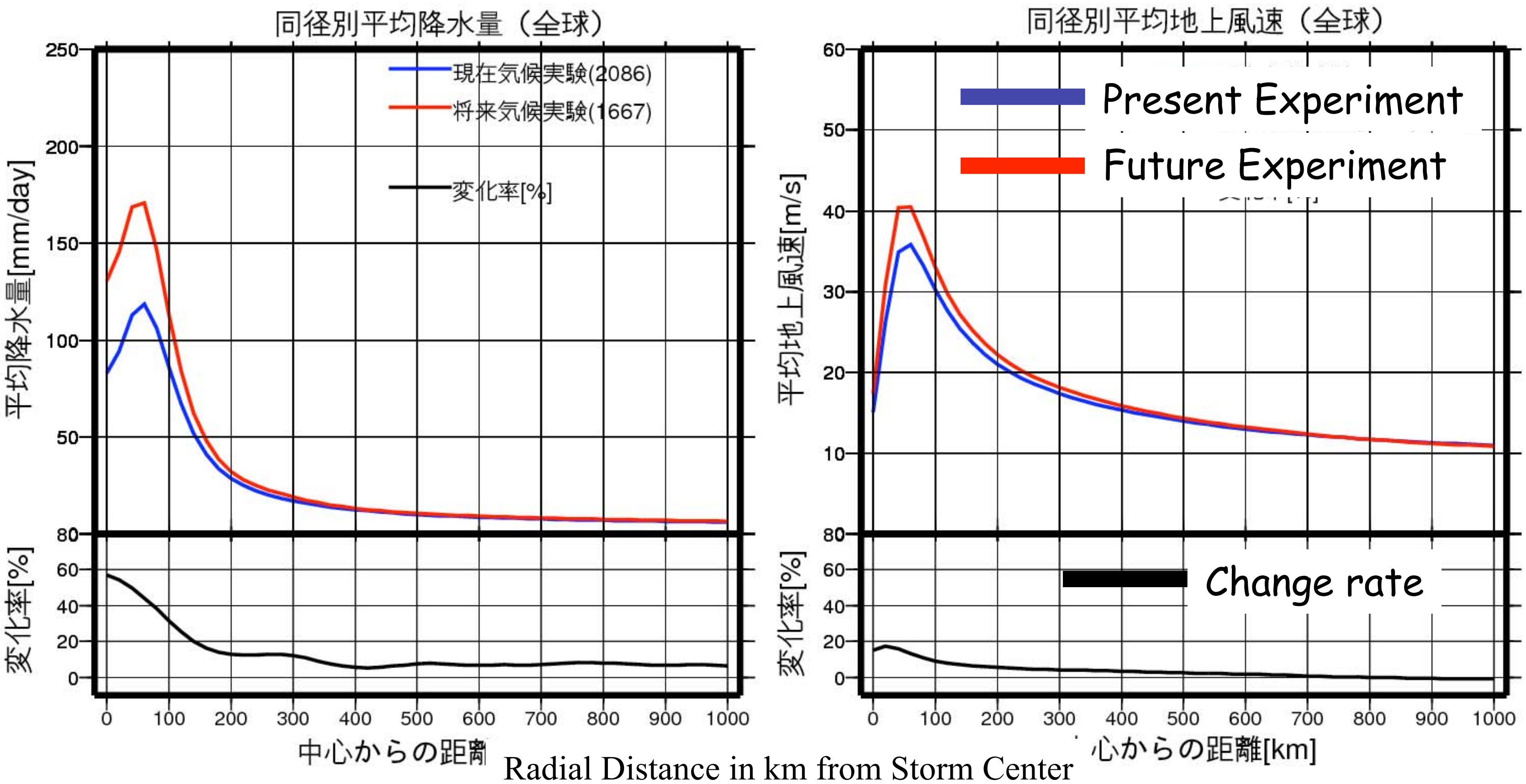

・Large changes occur near inner-core region, 40-60% for precipitation and 15-20% for surface wind.

・A surface wind speed increase of more than 4% can be seen up to 500 km from storm center.

Interprete TC track changes

Future change in frequency of TC occurrence

Present-day (1979-2003, Jul-Oct)

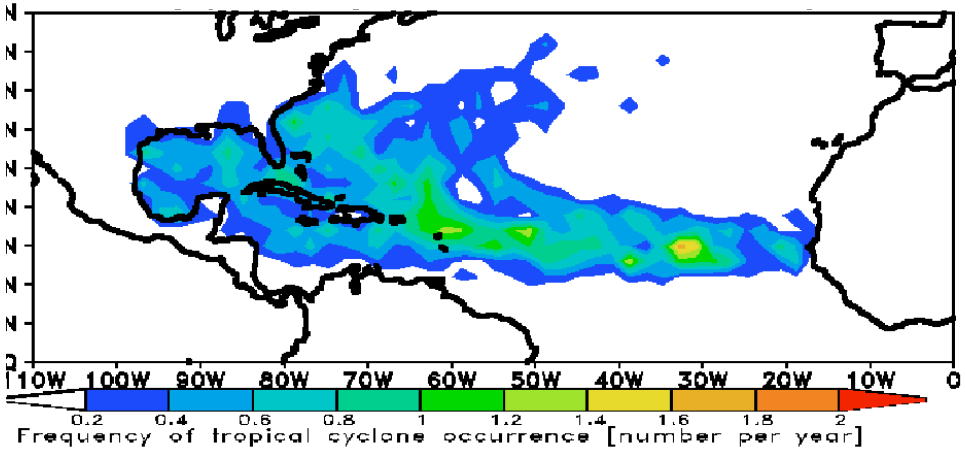

Future (2075-2000, Jul-Oct)

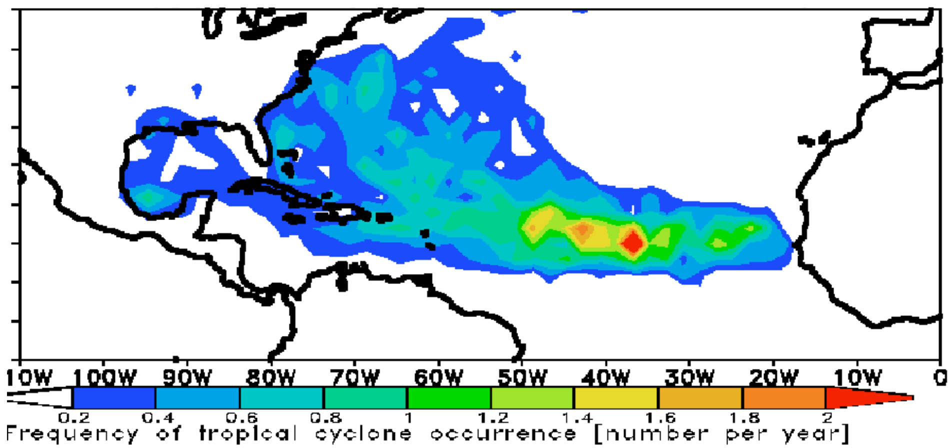

Future – Present-day (Jul-Oct)

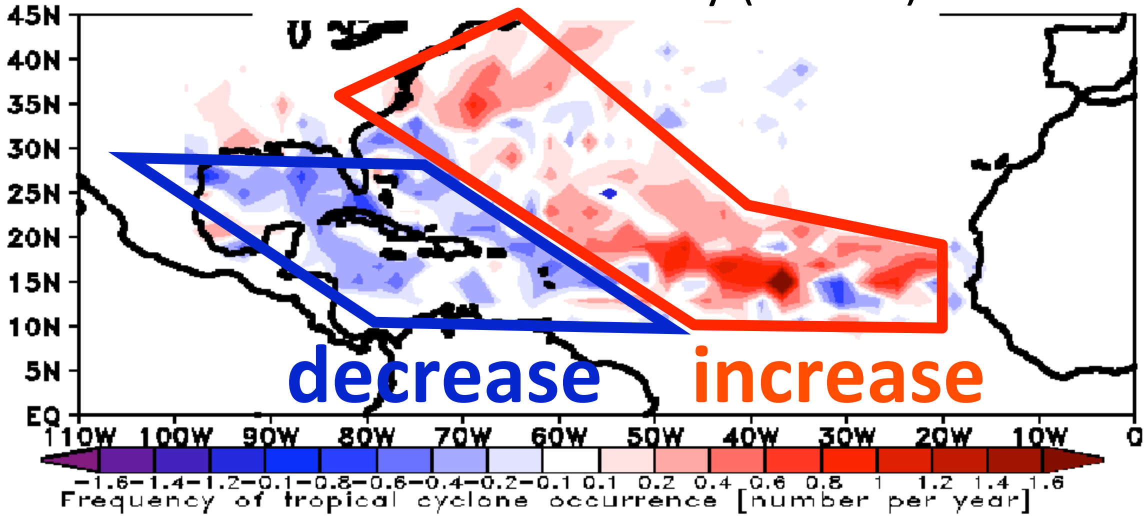

The TC frequency will decrease in the western North Atlantic and increase in the eastern North Atlantic

Reason for track change

Change in steering flow (Jul-Oct)

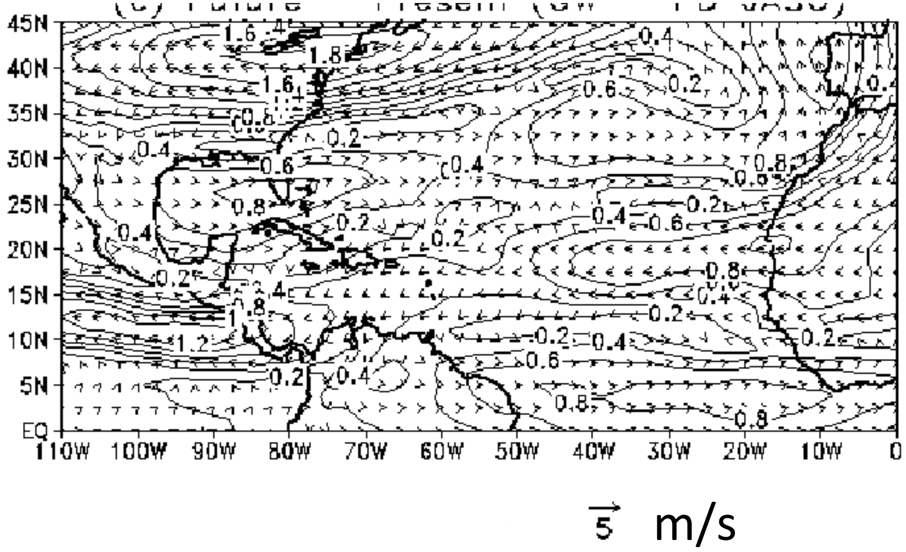

Change in frequency of genesis (Jul-Oct)

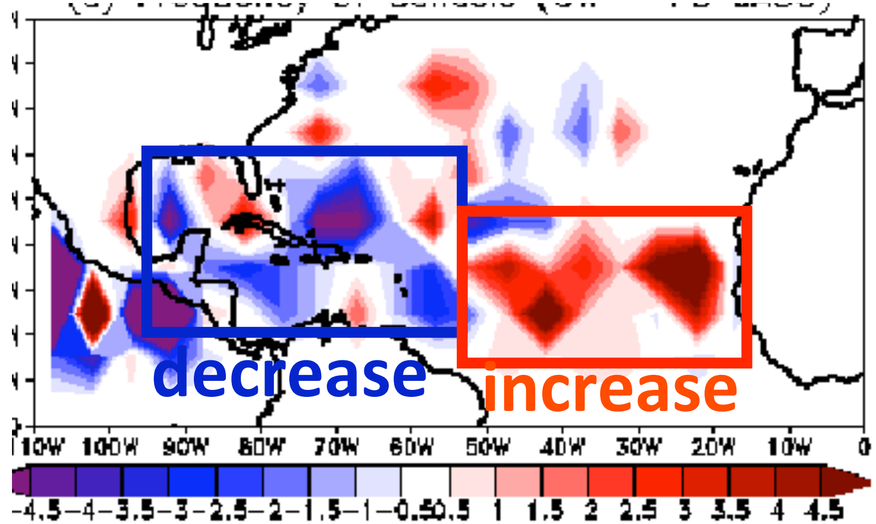

only a small difference in steering flows

Track changes are caused by alternation in TC genesis locations rather than in TC steering flows

Future change in Genesis Potential Index

$$GPI = \left|10^5 \eta\right|^{3/2} \left(\frac{R}{50}\right)^3 \left(\frac{V_{pot}}{70}\right)^3 \left(1 + 0.1 V_{shear}\right)^{-2} \left(\frac{-\omega + 0.1}{0.1}\right)$$

Absolute vorticity at 850 hPa

Relative humidity at 600 hPa

Maximum potential intensity

Vertical wind shear between 850 hPa and 200 hPa

Vertical velocity at 500 hPa

Change in frequency of genesis (Jul-Oct)

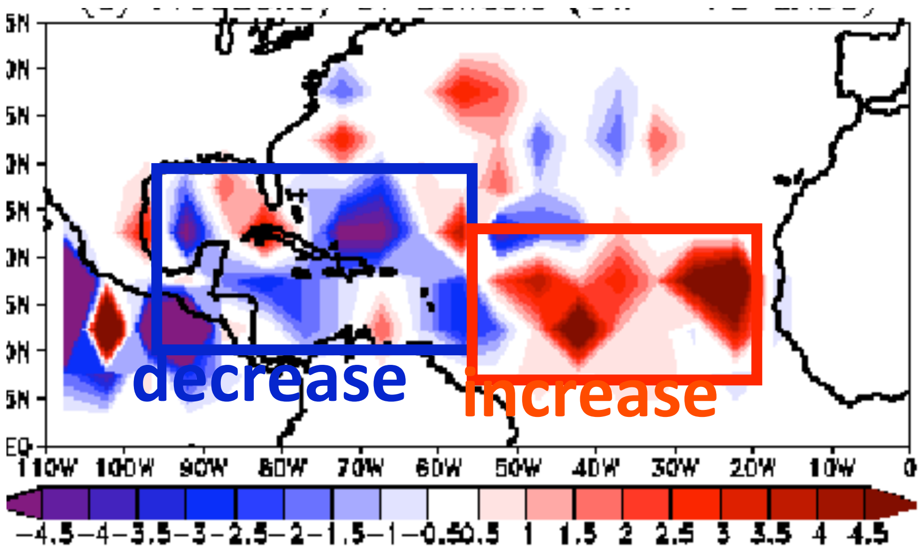

Change in GPI (Jul-Oct)

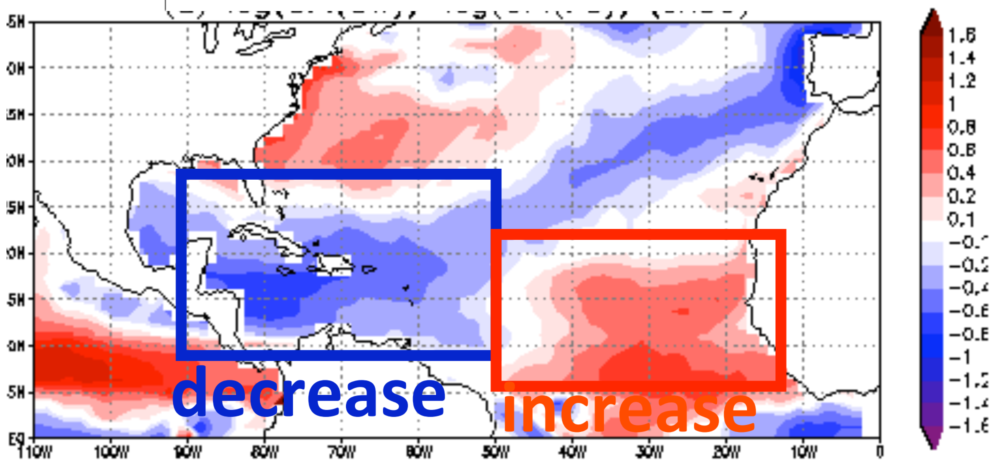

The GPI change correctly depicts the change in frequency of genesis

The GPI can be used to determine which of the GPI elements contribute most to its future change

Influential factor to the change in GPI

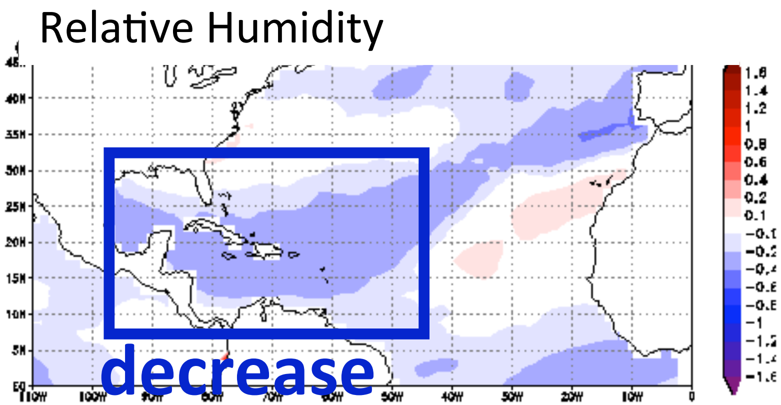

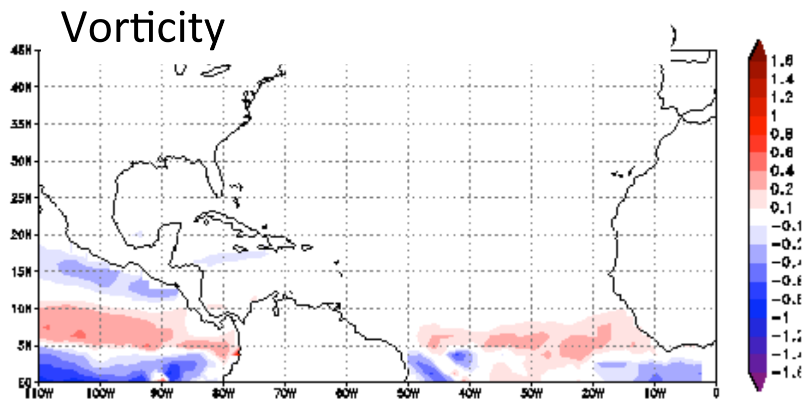

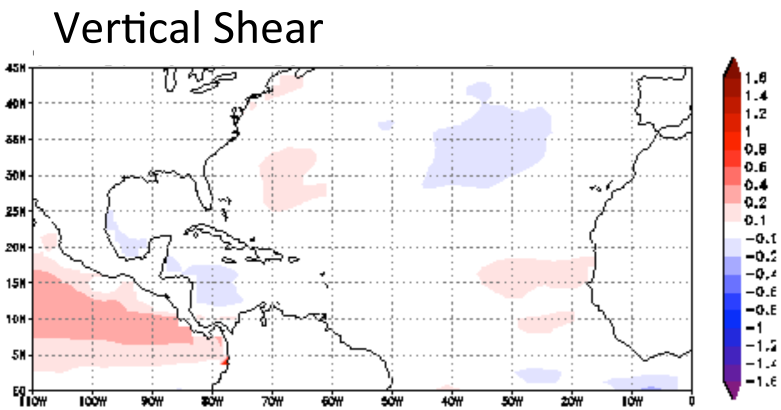

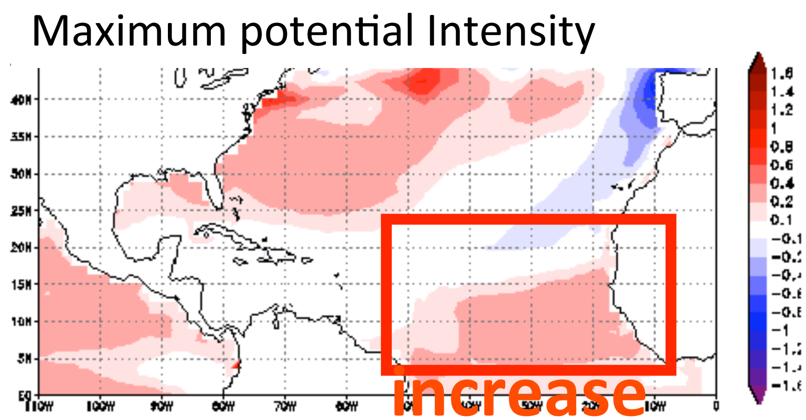

Changes in the maximum potential intensity and omega terms make the dominant contribution to the increase in the GPI within the eastern North Atlantic, whereas the relative humidity and omega terms make the largest contribution to the decrease in the GPI within the western North Atlantic

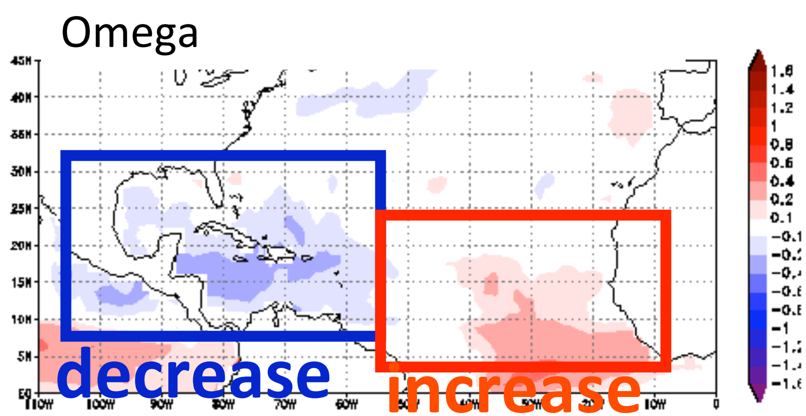

Reason for TC genesis change

Change in Omega (Jul-Oct)

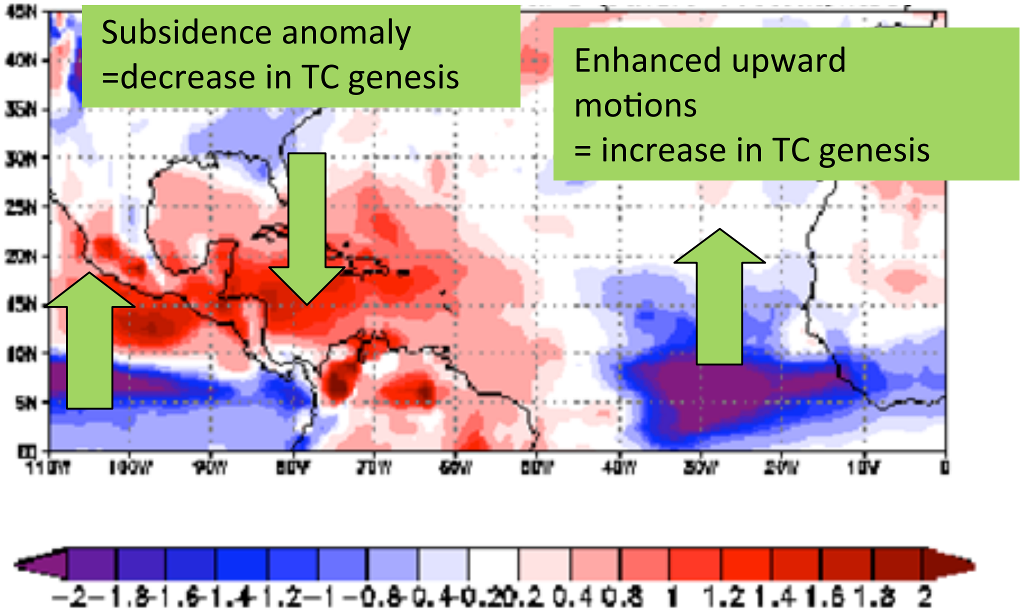

Change in prescribed SST (Jul-Oct)

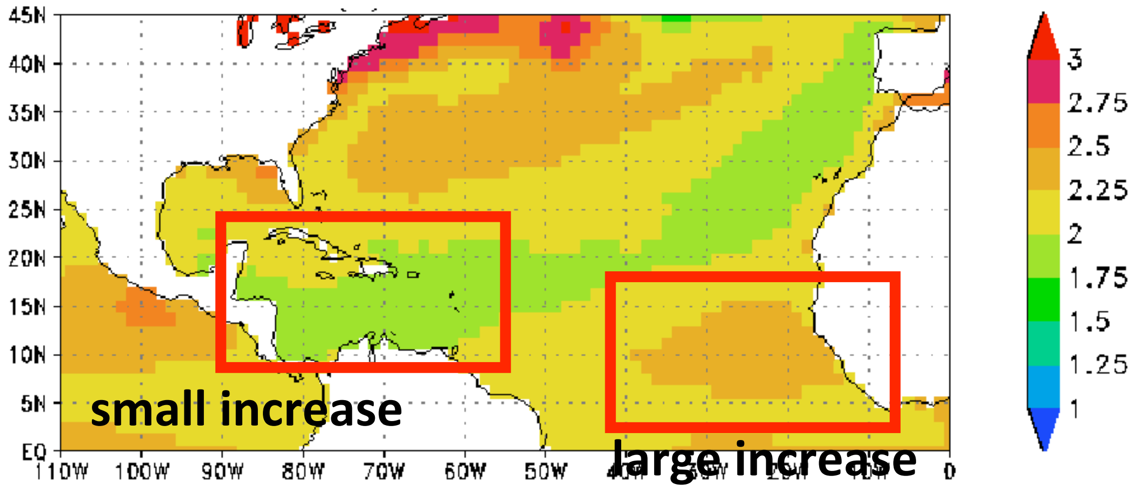

The reduction of genesis in the west North Atlantic is attributed to decreases in relative humidity and ascending motion caused by an enhanced large scale subsidence, whereas the increase of genesis in the southeast North Atlantic arises from increasing upward motion and convective available potential energy due to local ocean surface warming

Future change in frequency of TC occurrence

Present-day (1979-2003, Jul-Sep)

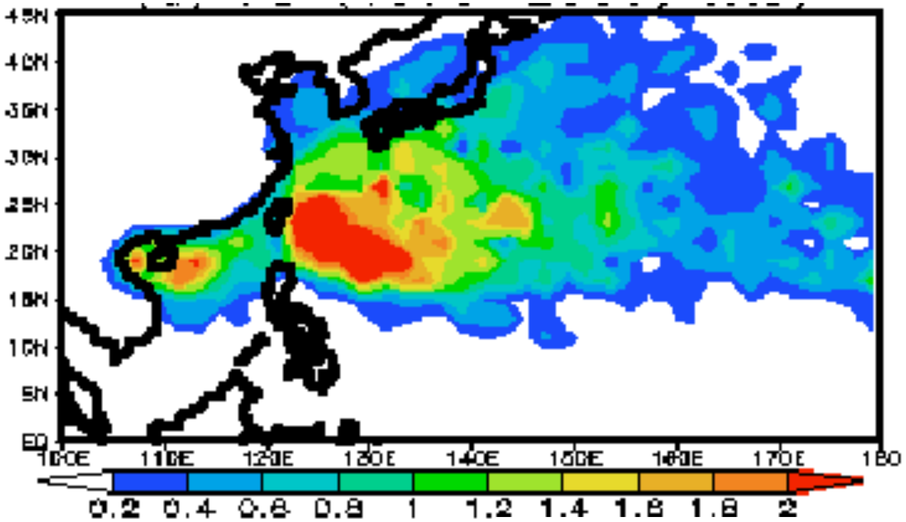

Future (2075-2000, Jul-Sep)

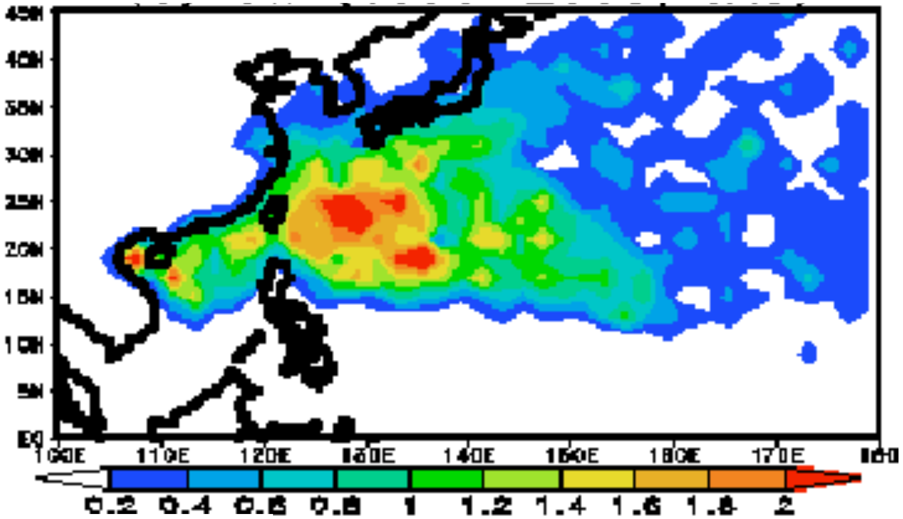

Future – Present-day (Jul-Sep)

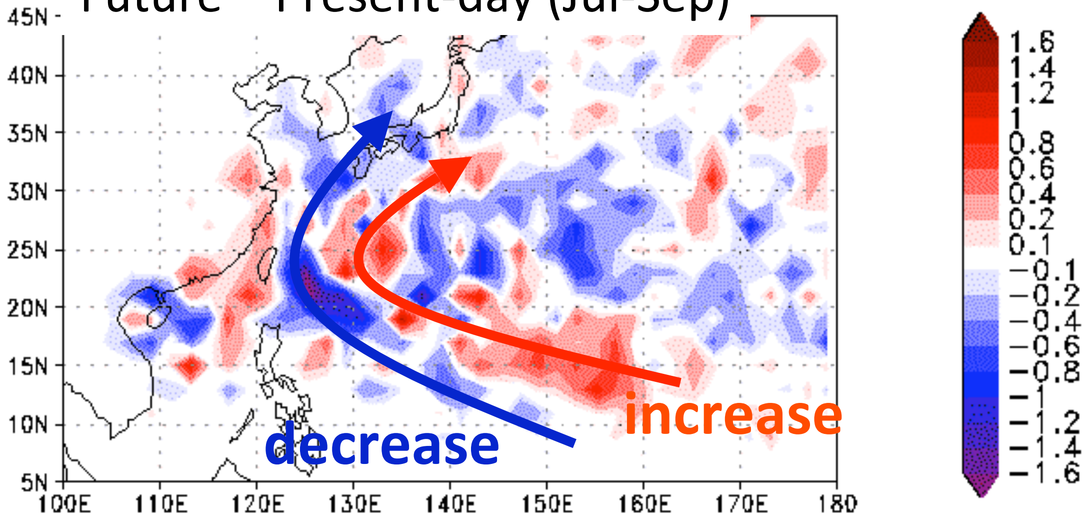

Frequency of TC landfall over Japan and Korea may decrease

Future change in tropical cyclone frequency with various resolutions and SST settings

Future change in TC frequency

Sugi et al. (2009)

The changes in tropical cyclone frequency as projected by 20km-mesh and 60-km-mesh global atmospheric model experiments. The changes are shown in terms of the ratio of future frequency to present frequency. Statistically significant increase (decrease) at 95%confidence level by two-sided t-test is indicated by red (blue) color.

Experiments	Resolution	_ SST	Integratioin	Ratio(%) of TC frequency Future/Present								
				Global	NH	SH	N Indian	NW Pacific	NE Pacific	N Atlantic	S Indian	S Pacific
A0	TL959, 20km	MRI CGCM2.3	20yr	71	69	73	61	64	61	122	72	77
A1		MRI CGCM2.3	20yr	75	75	75	71	71	70	123	75	73
A2		MIROC-H	10yr	73	85	58	132	128	50	82	76	11
A3		CMIP3	25yr	80	79	81	85	74	75	105	95	58
B1	TL319, 60km	MRI CGCM2.3	25yr	80	79	83	89	66	69	150	78	92
B2		MIROC-H	25yr	94	100	84	179	164	58	106	110	31
B3		CMIP3	25yr	79	81	76	133	86	67	104	79	64
B4		CSIRO	25yr	78	71	89	93	113	51	63	78	110
C3	TL159, 120km	CMIP3	25yr	71	79	54	99	75	78	75	62	38

Commonly reduced regardless of difference in SST increase pattern.

Mostly same changes are achieved by the same SST setting regardless of resolution difference.

Extratropical cyclones

Extratropical Cyclones

Total cyclone number

"Strong" cyclone number (<970hPa)

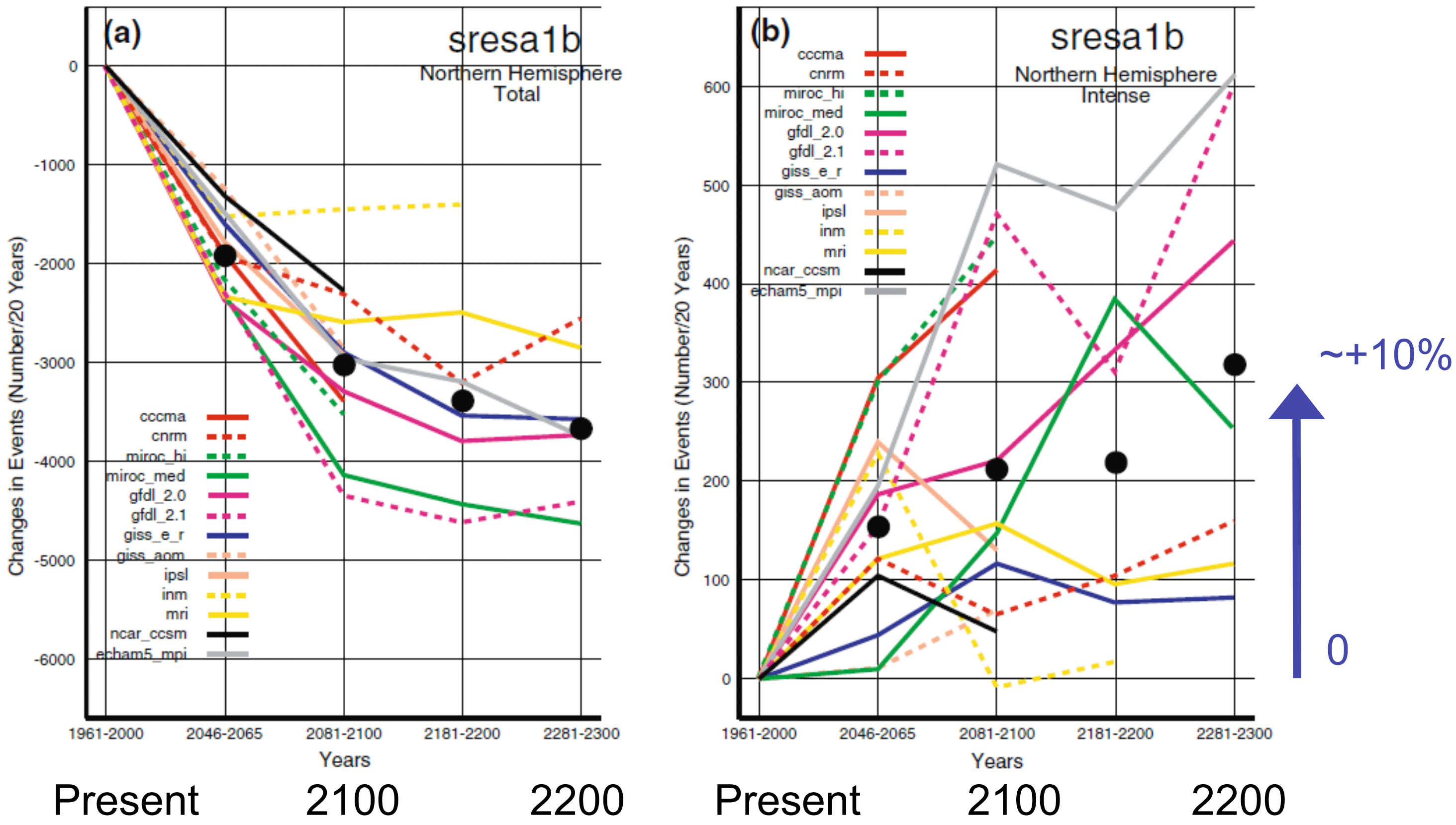

- **When tracking extratropical cyclones..**
  - **Number of cyclones decreases**
  - **"Strong" cyclones increase**

Lambert and Fyfe (2006)

Same in high-resolution models but with different threshold for + or -

MRI AGCM

Frequency of cyclones as a function of threshold pressure

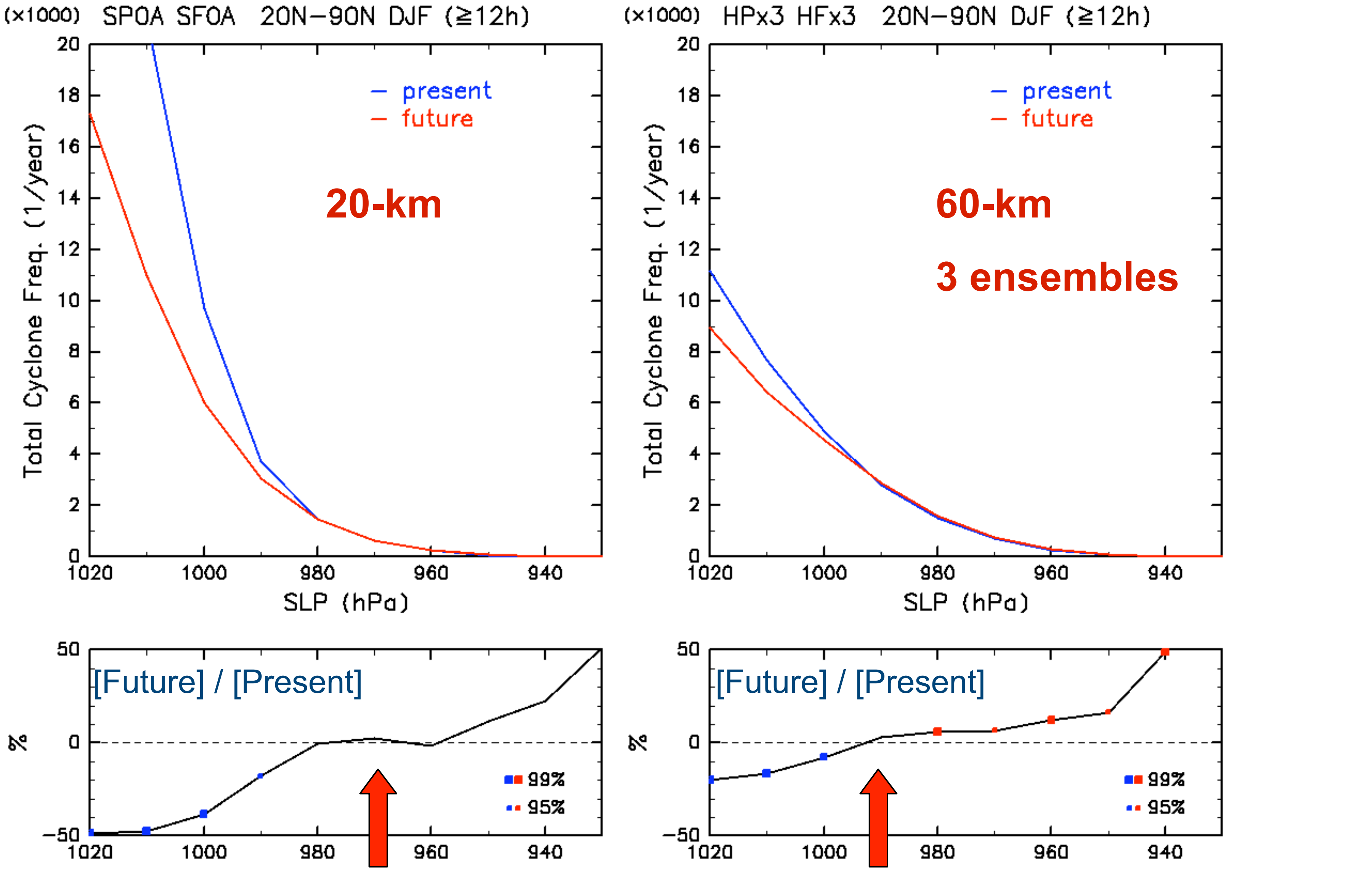

Mizuta et al. (2009)

MRI AGCM

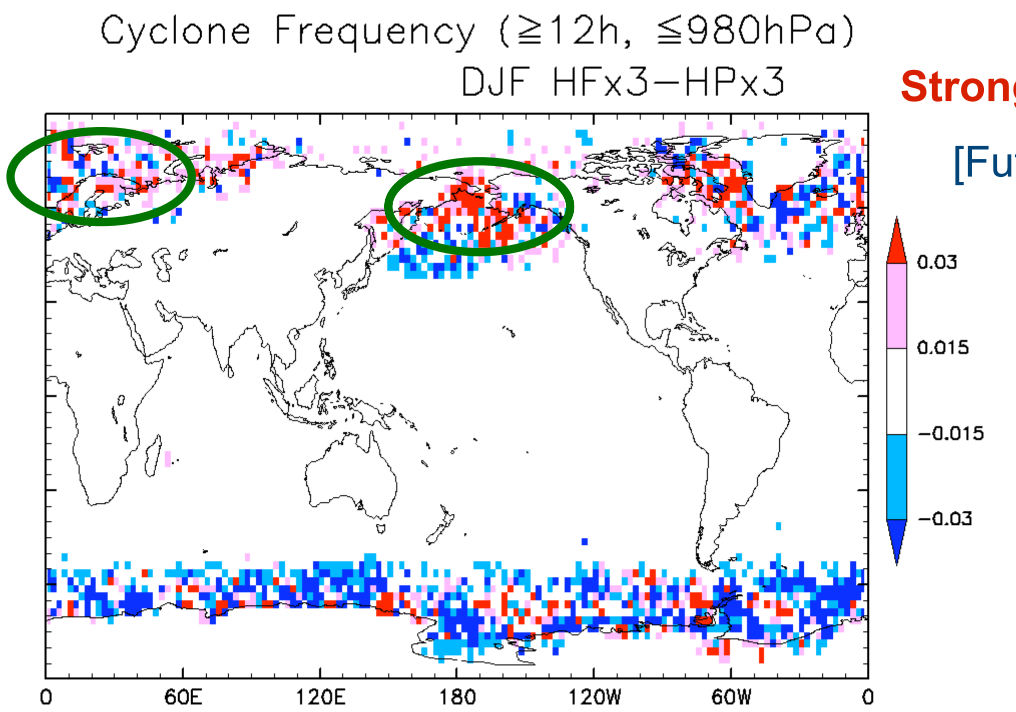

Strong Cyclone Frequency

[Future] - [Present]

Strong cyclones increase in the downstream of the storm tracks

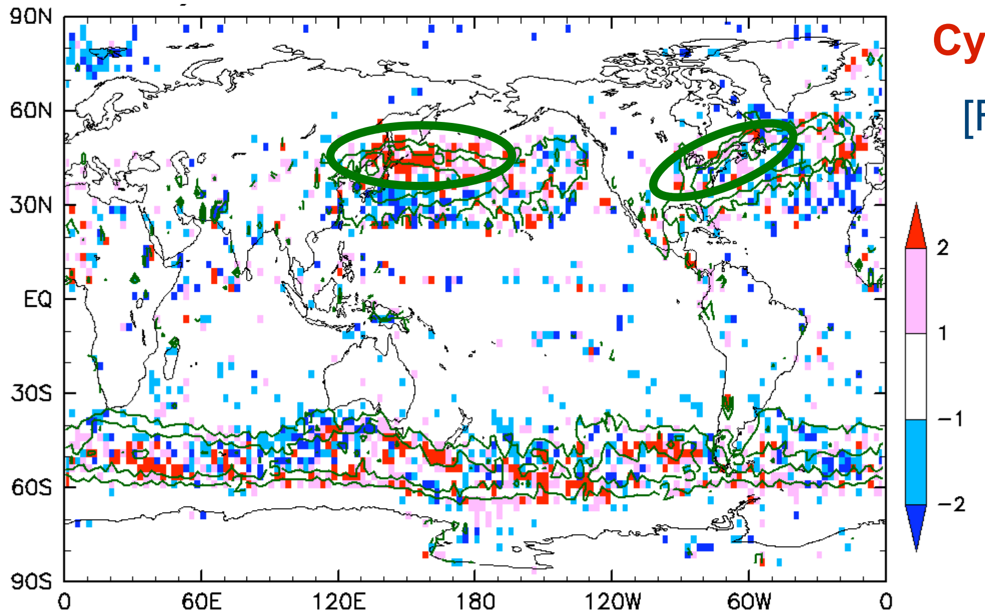

Cyclone Growth Rate

[Future] - [Present]

Growth Rate = temporal change of SLP along the track

$$\sigma_{SLP} = -(SLP_{t+} - SLP_{t-})$$

Increase in the upstream of strong cyclone increases

Mizuta et al. (2009)

Baroclinicity (maximum Eady growth rate; Lindzen and Farrell 1980)

$$\sigma_{\mathrm{BI}} = 0.31 g N^{-1} T^{-1} \nabla T$$

Increase at higher levels of polar region

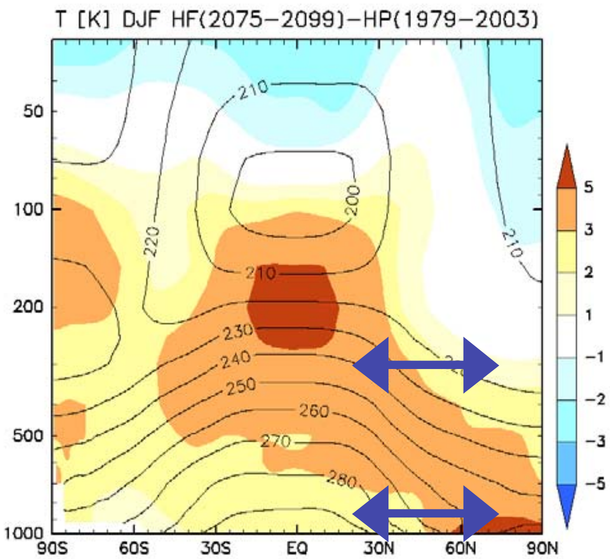

MRI AGCM

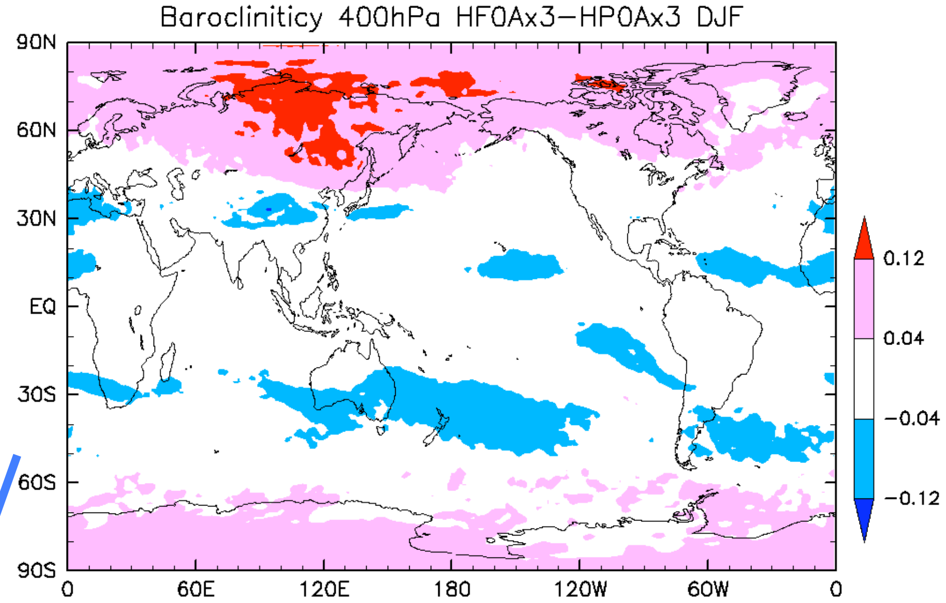

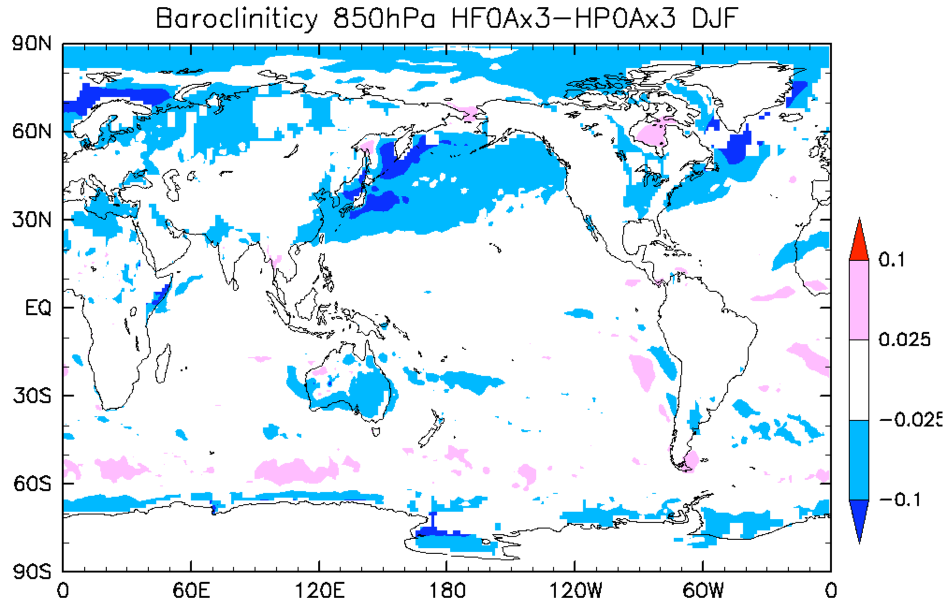

Mizuta et al. (2009)

Pattern correlation between the cyclone growth rate change and baroclinicity change (Pacific region)

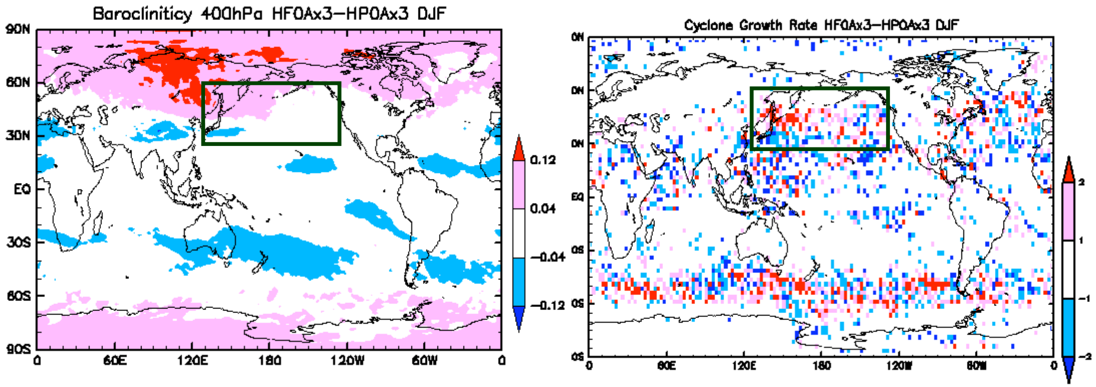

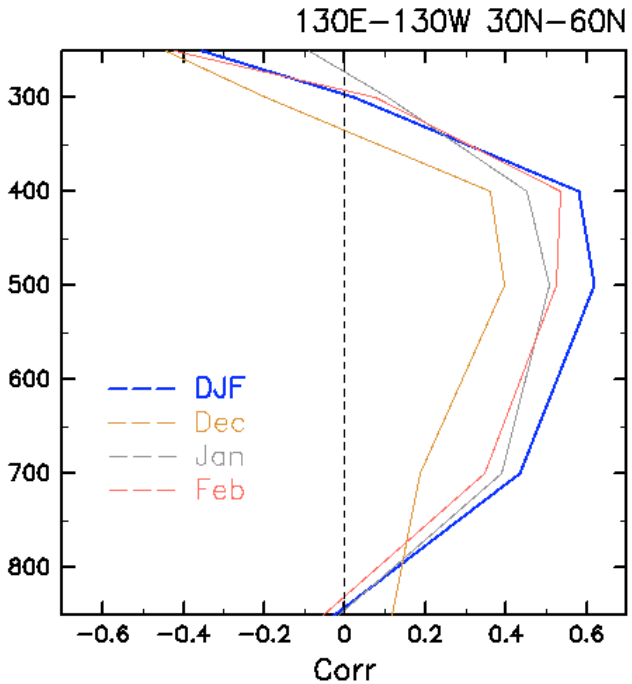

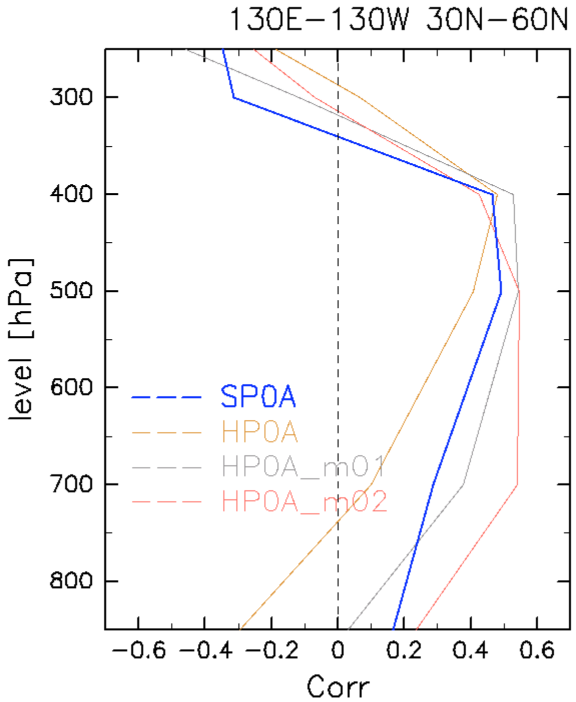

Each month of 3-member ensembles

DJF of each member

Mizuta et al. (2009)

NH winter blockings

Northern Hemisphere wintertime blocking

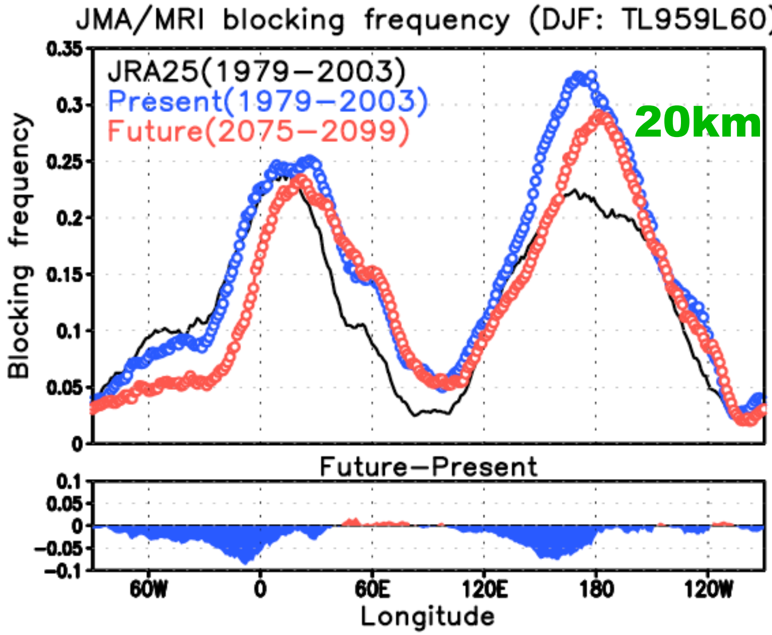

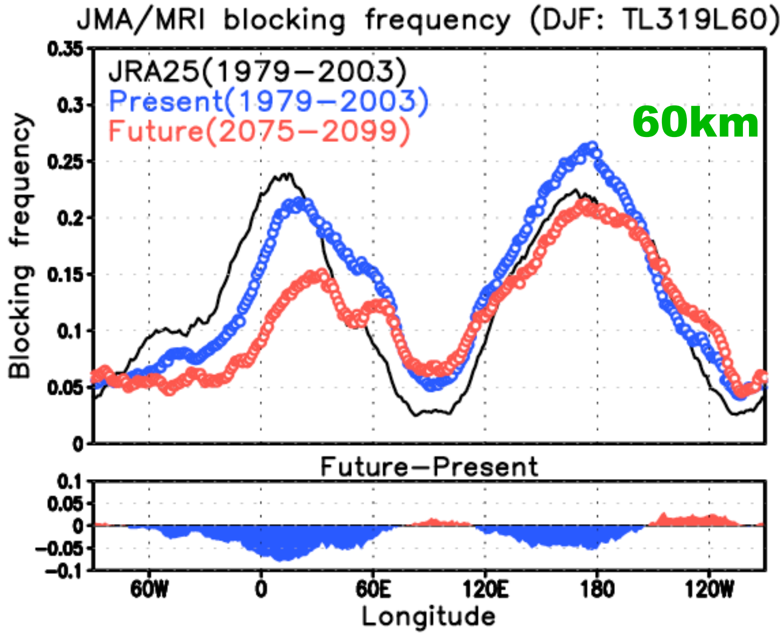

The higher the resolution, the more accurate the simulated Euro-Atlantic blocking frequency

Frequencies of Euro-Atlantic and Pacific blockings are projected to decrease

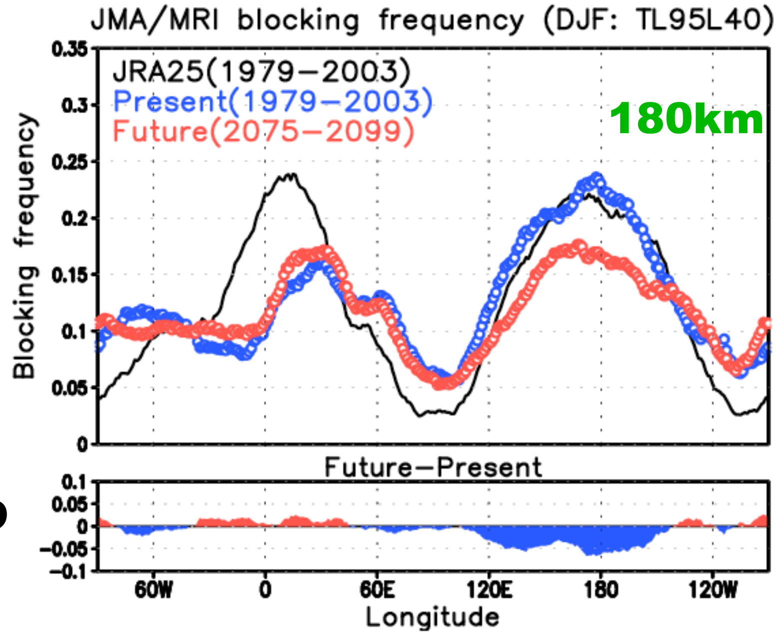

Matsueda et al. (2009) JGR

Uncertainty in future projections of blocking

60km ensemble simulations with different SSTs

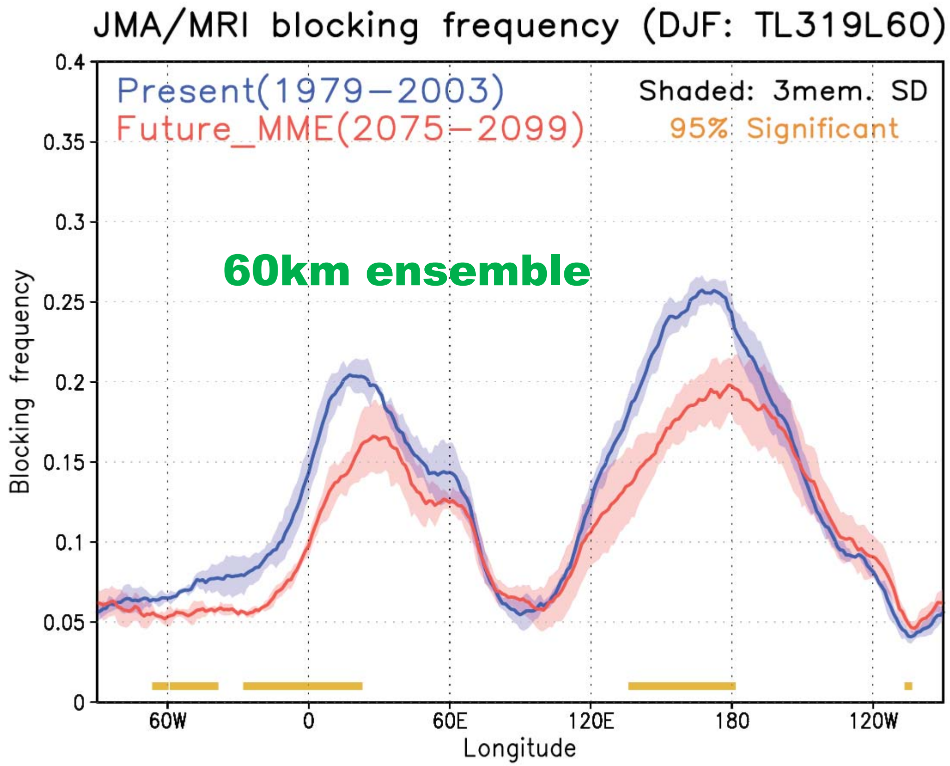

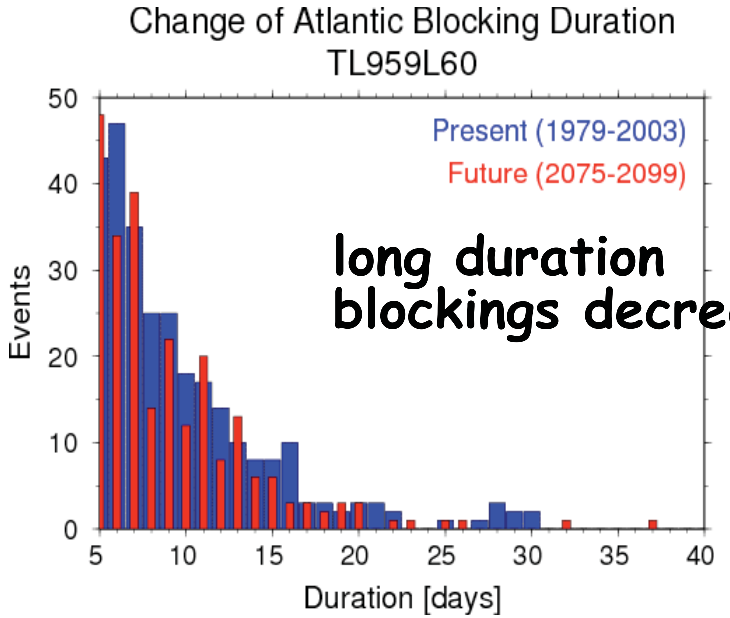

long duration blockings decrease

frequencies of Euro-Atlantic and Pacific blockings are projected to decrease significantly.

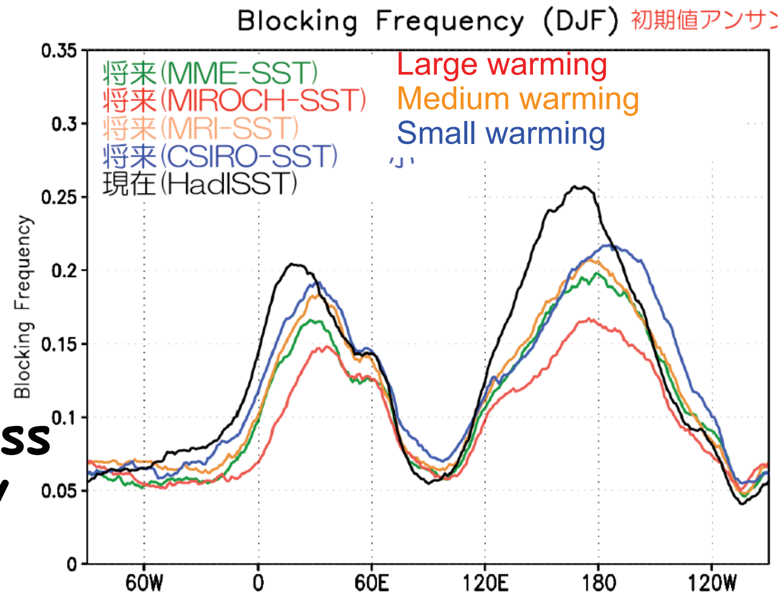

The larger the warming is, the less blocking frequency

Matsueda et al. (2009)

Summary

- High resolution model is needed to better represent weather extremes and tropical cyclones
- Topography is better represented by high resolution model
- Large-scale features of model climate improve by increasing horizontal resolution
- Resolution of climate models becomes finer; now we can use 60-km or even 20-km mesh global climate models
- Resolution vs ensemble is an issue
- Study to interpret and connect high-resolution and lower-resolution results (e.g. scaling) is needed
- Caveats: model bias, air-sea coupling

Further steps

Improvement of TC and precipitation

New Cumulus + Ocean Skin | OBS（Besttrack+CMAP） | Current Model

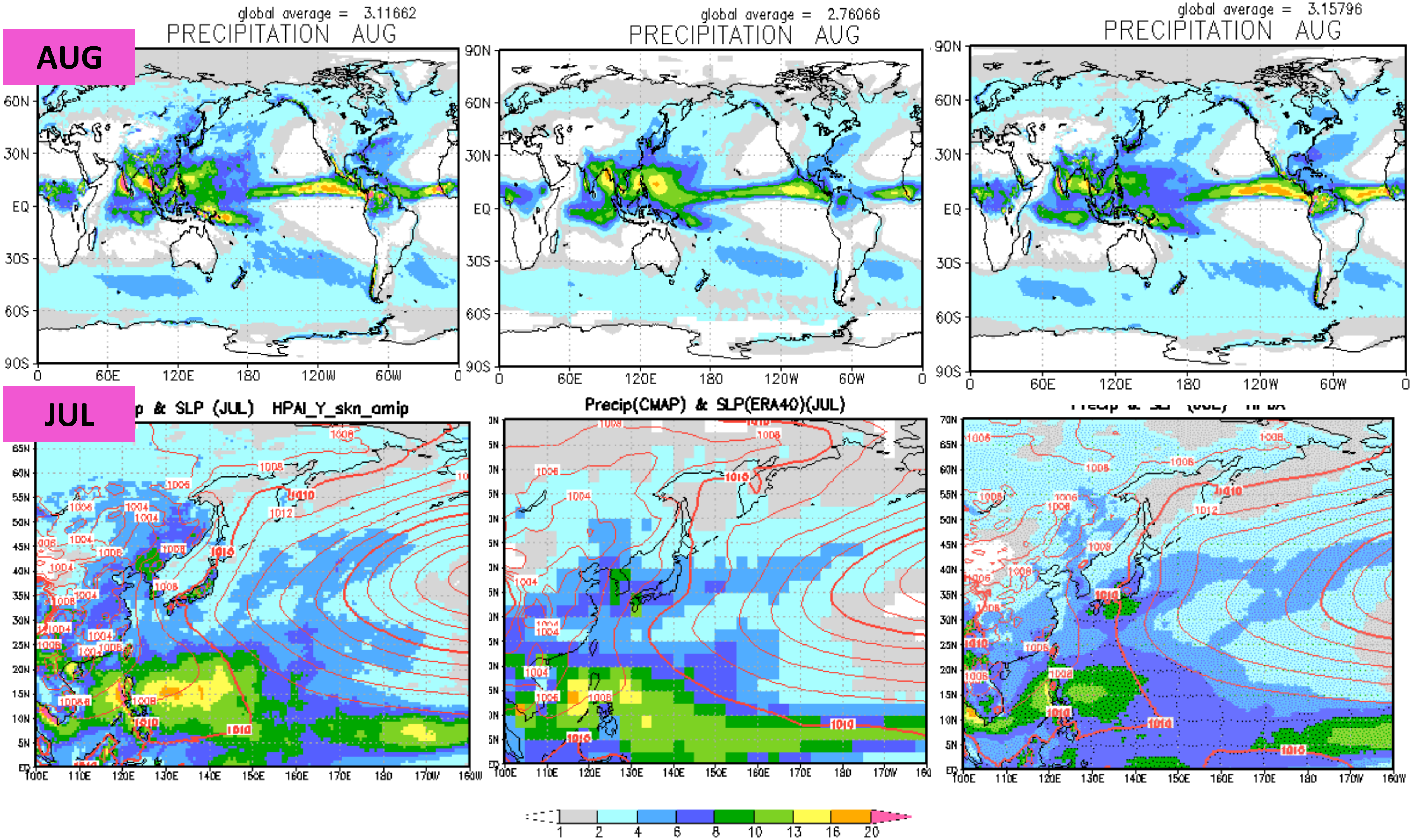

MRI Earth System Model: CMIP5 and after

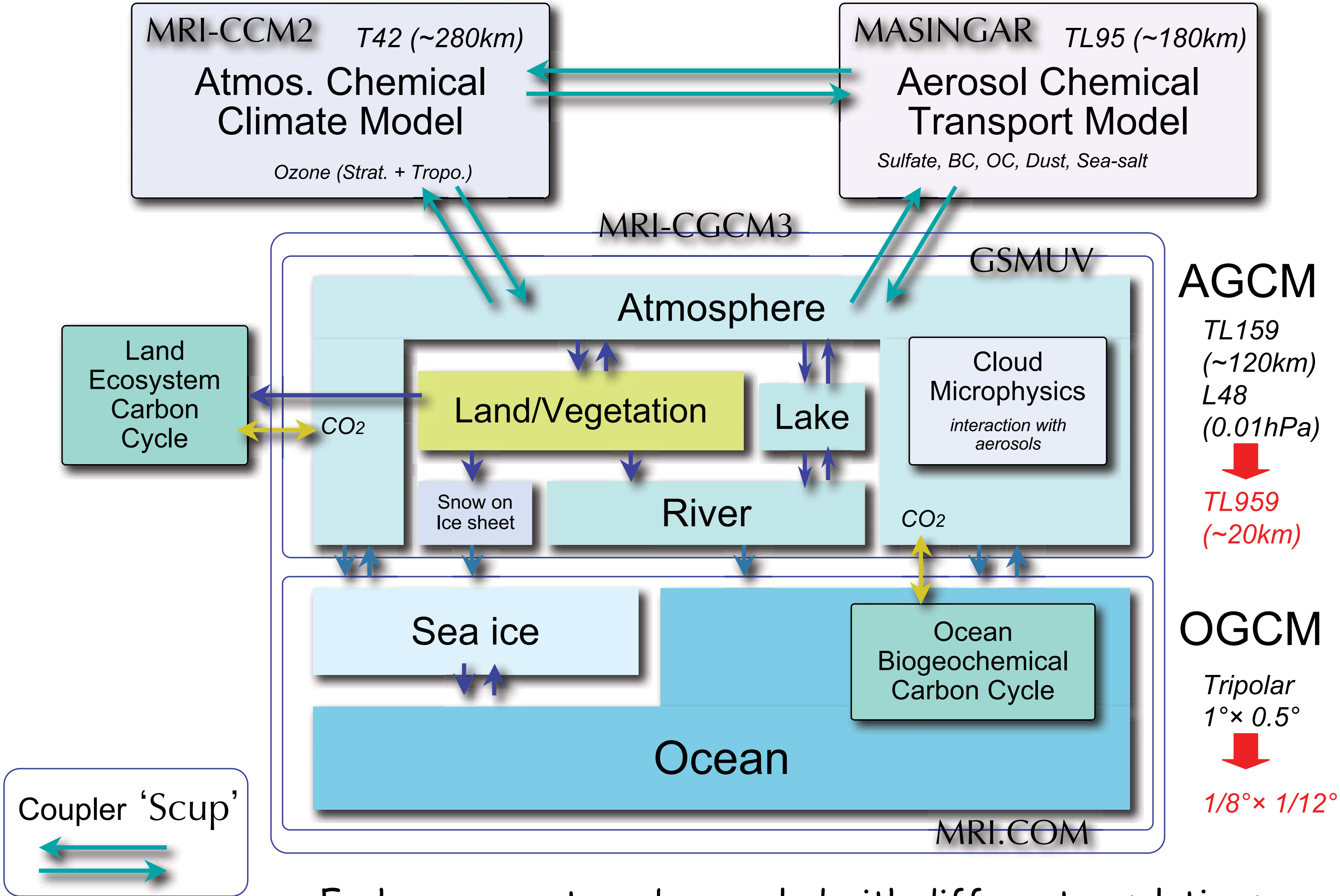

Each component can be coupled with different resolutions